Published in final edited form as:
Adv Healthc Mater. 2014 August ; 3(8): 1217–1221. doi:10.1002/adhm.201300645.

Supramolecular nanofibrils inhibit cancer progression *in vitro* and *in vivo*

Yi Kuang, **Xuewen Du**, **Jie Zhou**, and **Bing Xu**
Brandeis University, 415 South St., MS 015, Waltham, MA 02453

Abstract

The recent discovery of the inverse comorbidity between cancer and Alzheimer's disease implies that one may use amyloids to inhibit tumors. During the conversion of a dipeptide segment (Phe-Phe) in β-amyloid into a supramolecular hydrogelator, we obtained a small molecule (**1**) that can self-assembly into nanofibrils via multiple intermolecular hydrogen bonding and aromatic-aromatic interactions. Interestingly, while the monomers of **1** are innocuous, the nanofibrils formed by **1** can selectively inhibit the growth of glioblastoma cells over neuronal cells. To further assess the potential of this small molecular nanofibrils as anti-cancer agent, we exam the biological activity of the nanofibrils and demonstrate that the nanofibrils of **1** efficiently inhibit the progression of cancer cells (e.g., HeLa cells) both in cell assays and on xenograft mice model. This work suggests that nanofibrils derived from core motif of amyloid are effective agents for inhibiting cancer progression. Thus, this work contributes to a new approach that uses supramolecular nanofibrils as *de novo* molecular amyloids for inhibiting the growth of cancer cells.

Keywords

supramolecular; nanofibrils; anticancer; inverse comorbidity; *de novo* amyloid oligomer

This communication reports the use of nanofibrils formed by the small molecules cosisting of the core motif of amyloid as *de novo* molecular amyloids for inhibiting HeLa cells *in vitro* and in a mice model. Cancer[1] and Alzheimer's disease[2] are major threats to the public health. While both diseases are still being understood, epidemiological and clinical studies suggest that there is an inverse comorbidity between cancer and Alzheimer's disease.[3] The intriguing inverse association has stimulated the hope that the understanding of the mechanisms underlying the inverse association may lead to novel therapies for both diseases. In fact, after long debates about the causative agents of Alzheimer's disease, now it is suggested that soluble amyloid oligomers are the most neurotoxic species.[4] Recent studies also suggest that the early aggregates of misfolded non-disease-associated proteins[5] and oligomers of disease-associated proteins (e.g., Aβs)[6] exhibit similar inherent cytotoxicity. These results not only represent an important mechanistic advance on a

bxu@brandeis.edu.

Supporting Information
Supporting Information is available from the Wiley Online Library.

common mechanism of the cytotoxicity of the aggregates, but also imply that one may use these aggregates of peptides or proteins to induce apoptosis of cancer cells.[7]

Coincidentally, during our study of the aggregates of a small hydrophobic molecule, we constructed the molecular nanofibrils that are biophysically and morphologically resemble the aggregates of aberrant protein. For example, they all rely on extensive, non-covalent intermolecular interactions (i.e., supramolecular interactions) to form cross-β fibrillar aggregates in aqueous medium.[8] More importantly, we found that the molecular nanofibrils (denoted as "nanofibrils" in this article) disrupt the dynamics of microtubules, leading to apoptosis of glioblastoma cells.[7] Notably, those nanofibrils exhibit little acute toxicity towards a neuronal cell line (PC12).[7] Besides as the first example of the self-assembly of small molecules to disrupt self-organization of functional proteins, that work supports the further investigation of the nanofibrils as new type of agents for selective inhibition of cancer.

In this work, we demonstrate that the molecules of **1**, a conjugate of a core motif of amyloid (Phe-Phe)[8] and a naphthalene group, self-assemble to afford molecular nanofibrils, which exhibit higher physical and biological stability than its monomer. The nanofibrils of **1** not only sufficiently inhibit the growth of HeLa cells within 48 hours in cell assay, but also effectively inhibit the progression of xenograft tumor model of HeLa cells on a mice model. Importantly, the nanofibrils induce the death of cancer cells through apoptosis of HeLa cells, thus exerting little side effects to the normal tissues on the mice. These results suggest that supramolecular nanofibrils can serve as a new type of anti-cancer agents. Moreover, as *de novo* molecular amyloids, the anti-cancer property of the nanofibrils provides a new approach for exploring the inverse comorbidity between cancers and neurodegenerative diseases, which ultimately may lead to a new paradigm in cancer therapy, as well as in the treatment of neurodegenerative diseases.

The peptide derivative **1**, synthesized by solid phase peptide synthesis (SPPS), consists of a diphenylalanine (a core motif of amyloid (Aβ)[9]) and a naphthalene moiety (Scheme 1, Figure S1)). The inclusion of phenyl and naphthyl groups enhances aromatic-aromatic interactions for molecular self-assembly in water.[10] In the previous work, we have demonstrated that the critical concentration for self-assembly of **1** in PBS buffer is around 154 to 163 μg/mL.[7] As shown in Figure 1A, the negatively-stained transmission electron microscopy (TEM) image reveals that, above this critical concentration, the PBS buffer with **1** ([**1**] = 192 μg/mL; pH 7.6) contains nanofibrils that have uniform width at 24±2 nm. The circular dichroism (CD) spectrum of the solution shows a negative peak at 190 nm followed by a positive peak at 200 nm. The peptidic component of **1** permits the analysis of the CD spectrum of the solution (Table S1) by a CD simulation software[11]. The spectra of two independent batches of solutions are both in accord with the ordered β-sheet structure of proteins, indicating that the molecular assemblies of **1** adopt β-sheet-like interactions to form nanofibrils. In addition, as culture medium (MEM with 10% FBS, 1% antibiotic) is a different buffer system supplemented with amino acids and proteins, we also use TEM to examine the nanofibrils of **1** in the complete culture medium. Figure 1B shows that, at [**1**] = 192 μg/mL, nanofibrils (21±4 nm) also exist in culture mediums. These results warrant the nanofibrils of **1** to be administrated to HeLa cells in complete culture medium.

To evaluate the thermodynamic stability of the nanofibrils in solution, we measured the dilution enthalpy of **1** by titration of the solution containing **1** into PBS buffer (Figure 1C). The enthalpy of dilution of **1** (ΔH_{dil}) is a negative value, indicating the exothermic (release of heat) dilution of **1**. The magnitude of the ΔH_{dil} of **1** increases with the increase of the concentrations of **1** up to 144 μg/mL (below critical self-assembly concentration), which follows the modified McMillan-Mayer model that states the ΔH_{dil} is a monotonic function of the effective concentration of the solute.[12] At [**1**] = 192 μg/mL, above the critical self-assembly concentration, the ΔH_{dil} of **1** abruptly drops instead of increases, which drastically departs from the trend and is the smallest value measured. As shown Figure 1C, the ΔH_{dil} at [**1**] = 192 μg/mL (results from the dilution of monomers and nanofibrils of **1**) is smaller than the ΔH_{dil} at [**1**] = 48 μg/mL (results from the dilution of monomers of **1** alone). In other words, the nanofibrils of **1**, after formation, unlikely dissolve quickly when being diluted. Thus, the nanofibrils of **1** possess significant kinetic stability (i.e., half-life should be longer than the time scale of ITC experiment).

To assess the biochemical stability of the nanofibrils of **1** inside the cells, we measured the intracellular degradation of the monomers and the nanofibrils of **1** by incubating HeLa cells with [**1**] at 144 μg/mL or 192 μg/mL for 12 h. Figure 1D shows the intracellular concentration of **1** and the proteolytic remnant of **1** of which the second Phe is cleaved due to the hydrolysis of amide bond. Upon 12 h of incubation, **1** accumulates in the HeLa cells treated with [**1**] at 144 μg/mL or 192 μg/mL. A small amount of proteolytic remnant of **1** also appears in those HeLa cells. However, there is a difference in the calculated average degradation rate (R = the amount of proteolytic remnant/the intracellular amount of **1**). R of cells treated with [**1**] at 144 μg/mL is 0.134, which is larger than that of cells treated with [**1**] at 192 μg/mL (R = 0.119). The lower degradation rate at [**1**] = 192 μg/mL indicates the higher biostability of the nanofibrils of **1** comparing with its monomers, suggesting that the nanofibrils of **1**, as individual entities, structurally and biochemically differ with the monomeric **1**. Apparently, peptidases process the nanofibrils of **1** more slowly that to the monomeric **1**. The excellent kinetic and the biochemical stabilities of the nanofibrils of **1** satisfy the prerequisites for them to serve as supramolecular nanostructure for inhibiting cancer cells.

The physiochemical and biochemical stability of the nanofibrils of **1** warrant a meaningful cell test of the nanofibrils. In our previous work, we have found that while the monomers of **1** ([**1**] = 96 or 144 μg/mL) are innocuous to cells, the nanofibrils of **1** ([**1**] = 192 or 240 μg/mL) exhibit cytotoxicity towards cancer cells (e.g., T98G, U78MG).[7] As shown in Figure 2, below the critical concentration of self-assembly, **1** exhibits little cytotoxicity towards HeLa cells; above the critical concentration of self-assembly, **1** significantly decreases the viability of the HeLa cells (to less than 20% within 48 h). Moreover, **2** (i.e., the enantiomer of **1**, formed by the replacement of the L-Phe-L-Phe with D-Phe-D-Phe), which has similar self-assembly property of **1**,[8] also exhibits cytotoxicity to HeLa cells at 192 or 240 μg/mL (Figure 2). Moreover, tubulin tracker revealed that the nanofibrils of **1** induce cytotoxicity on HeLa cells through disruption of the dynamic of microtubules.[7] Similarly, **2**, at and above 192 μg/mL, also disrupts the elongation of microtubules (i.e., resulting in clustered short microtubules, in Figure S2). The same cytotoxicity and similar

microtubule disruption of **1** and **2** exclude the possibility that the monomer of **1** or **2** acts as a specific ligand for unknown receptors to result in the cell death. These results support that the cytotoxicity of **1** towards cancer cells, above the critical concentration of self-assembly, stems from the formation of nanofibrils of **1** at these concentrations. Moreover, the result of **2** indicates that the cytotoxicity of nanofibrils of **1** is less dependent on the chirality of the peptides, similar to the report by Pastor *et al*. on the cytotoxicity of amyloid.[13]

We used FITC conjugated annexin V and propidium iodide (PI)[14] to determine the process of cell death induced by the nanofibrils of **1**. The membrane impermeable PI discriminates live or early apoptotic cells from late apoptotic or necrotic cells that lose membrane integrity. FITC conjugated annexin V stains both apoptotic cells, which expose phosphatidylserine extracellularly, and necrotic cells, which lose membrane integrity. Figure 3 shows the staining of the HeLa cells treated by nanofibrils of **1** ([**1**] = 192 μg/mL) for 36 h. Unlike living cells that exclude both dyes (first row, Figure 3) and necrotic cells (induced by incubation with 10% DMSO for 24 h) that stained by both dyes (third row, Figure 3), the HeLa cells treated by nanofibrils of **1** exclude PI, but allow FITC annexin V to stain their plasma membranes (second row), indicating that the HeLa cells treated by nanofibrils of **1** enters early apoptotic stage at 36 h. Agreeing with the finding in our previous work that the nanofibrils of **1** induce apoptosis on T98G cells,[7] these results also indicate that the nanofibrils of **1** induce apoptosis of cancer cells could be a general phenomenon.

Apoptosis, unlike necrosis, induces much less side effects to the surrounding tissues so we examined the *in vivo* anti-tumor ability of the nanofibrils of **1**. We inoculated HeLa cells on immune deficient mice (nu/nu mice)[15] and treated the xenograft tumors by peritumoral injection of the nanofibrils of **1** (starting on day 1 (which is 30 days after tumor inoculation; one injection in every three days; six injections) (Scheme 1B). As shown in the tumor progression curve (Figure 4A), the treatment of mice by **1** at 10 mg/kg (injection of 100 μL of PBS containing **1** at 2.4 μg/μL) starts to inhibit tumor progression notably after 1 dose (4 days) and the inhibition of progression become significant after 3 doses (10 days). On and after the 10^{th} day of treatment, there is significant difference in the relative tumor volume between the mice on control group (injection of 100 μL of PBS) and the mice treated by **1** at 10 mg/kg ($p < 0.05$, Student's test). At the end of the treatment (the 19^{th} day), the mice in the control groups all bear tumors that are at least 10 times bigger than that on the 1^{st} day, while the tumors on mice treated by **1** at 10 mg/kg has an average size almost identical to that on the 1^{st} day. The appearance of mice on the 19^{th} day of treatment evidently shows the inhibitory effect of **1** at 10 mg/kg (Figure 4C). Tumors on the mice from the group treated by 10 mg/kg of **1** are significantly smaller than the tumor on mice from the group treated by 1 mg/kg of **1** (injection of 100 μL of PBS containing **1** at 0.24 μg/μL) and the control group. Differ with the results in cell-based cytotoxicity assay, which show that the nanofibrils at 192 μg/mL decrease the viability of the HeLa cells to less than 20%, the nanofibrils at 10 mg/kg can inhibit the progression of the HeLa tumors on the animal models. The different efficacies of the nanofibers *in vitro* and *in vivo* agrees with the trend of the efficacy of other anti-cancer drug (e.g., paclitaxel has an IC_{50} of 2.6 nM to HeLa cells *in vitro*[16], and it slows the progression of tumor *in vivo* at 10 mg/kg[17]). Moreover, the skins covering and around the tumor appear to be normal (i.e., without ulceration or sclerosis)[18] on every mice

treated with **1**, and their body weights are comparable with the mice in control group (Figure 4B). This result is in accord with the histological staining of tissue of injection site of mice subcutaneously injected by a high dosage of **1** (4.8 mg/mL; 1 mL), which shows no notable sign of inflammation (Figure S3). These results indicate that subcutaneous injection of the nanofibrils of **1** unlikely elicit inflammatory response in the surrounding tissue of the mice or cause any severe side effects.

It is also worth noting that the formation of nanofibrils is important for the observed cytotoxicity of the aggregates. For example, compounds **3** (the second L-Phe in **1** substituted by D-Phe) and **4** (the first L-Phe in **1** substituted by D-Phe), two other stereochemical isomers (**3** and **4**) of **1**, possessing poor ability of self-assembly and resulting in neither nanofibrils nor a hydrogel, exhibit quite different bioactivities (Figure S4) with those of **1** and **2**. For example, **3** starts to show cytotoxicity towards HeLa cells at 24 h of incubation (e.g., IC_{50} = 216.5 μM), while **4** only exhibits moderate cytotoxicity at 72 h of incubation (e.g., IC_{50} = 153.1 μM). In addition, the cytotoxicity of **3** and **4** both follow the sigmoidal dose response law, suggesting that the cytotoxicity likely originates from the increase of the monomer concentration of **3** or **4**.[19] TEM of the solution of **3** at 240 μg/mL reveals major morphology as small aggregates with irregular shape, TEM of the solution of **4** at 240 μg/mL reveals major morphology as sphere-like aggregates. These results, agreeing with our previous finding that the morphology of self-assembled nanostructures dictates their interaction with cellular proteins,[20] suggest the morphology of the molecular aggregates plays a key role to induce apoptosis.

In conclusion, this work demonstrates that nanofibrils formed by a derivative of small peptides for inhibition of tumor progression both *in vitro* and *in vivo*. Particularly, the successful inhibition of tumor progression in the xenograft animal model underscores the potential of supramolecular nanofibrils as *de novo* amyloid oligomers for cancer therapy. Unlike the previous report,[7] which focuses on the selectivity of nanofibrils against cancer cells *in vitro*, this work presents the first study on anti-cancer activity of self-assembled nanofibrils on an animal model. The successful inhibition of tumor progression *in vivo* not only demonstrates the peritumoral injection as a feasible method for the study of self-assembled nanostructures, but also illustrates the potential of the nanofibrils to act as anti-cancer agents. Unlike Aβ oligomers that resist degradation and accumulate to induce chronic cytotoxicity, the degradation of **1** and other molecular aggregates are rather fast and even tunable.[21] The ability to control the spatiotemporal profiles of the molecular nanofibrils based on the self-assembly of small peptides not only offers a new dimension to control the cytotoxicity of aggregation, but also promises reduced chronic side effect. Moreover, although it remains challenge to provide a simple notion for explaining the lowered Alzheimer's disease rate in cancer patients, this study on the nanofibrils of **1** offers valuable insights for understanding the lowered cancer rate in Alzheimer's disease patients. While other possible molecular mechanisms certainly remain to be elucidated, this study offers a new perspective and a new direction for understanding and treating cancers.

Supplementary Material

Refer to Web version on PubMed Central for supplementary material.

Acknowledgments

This work was partially supported by NIH (R01CA14274) and MRSEC (DMR 0820492). We thank Brandeis University EM facility.

Reference

[1]. Eheman, C.; Henley, SJ.; Ballard-Barbash, R.; Jacobs, EJ.; Schymura, MJ.; Noone, A.; Pan, L.; Anderson, RN.; Fulton, JE.; Kohler, BA.; Jemal, A.; Ward, E.; Plescia, M.; Ries, LAG.; Edwards, BK. Cancer. Vol. 118. American Cancer Society; Atlanta: 2012. p. 2338anonymous2012

[2]. Brookmeyer R, Johnson E, Ziegler-Graham K, Arrighi HM. Alzheimers. Dement. 2007; 3:186. [PubMed: 19595937]

[3]. Driver JA, Beiser A, Au R, Kreger BE, Splansky GL, Kurth T, Kiel DP, Lu KP, Seshadri S, Wolf PA. Br. Med. J. 2012; 344:1442.Roe CM, Behrens MI, Xiong C, Miller JP, Morris JC. Neurology. 2005; 64:895. [PubMed: 15753432] Tabares-Seisdedos R, Dumont N, Baudot A, Valderas JM, Climent J, Valencia A, Crespo-Facorro B, Vieta E, Gomez-Beneyto M, Martinez S, Rubenstein JL. Lancet Oncol. 2011; 12:604. [PubMed: 21498115]

[4]. Oda T, Pasinetti GM, Osterburg HH, Anderson C, Johnson SA, Finch CE. Biochem Bioph Res Co. 1994; 204:1131.

[5]. Bucciantini M, Giannoni E, Chiti F, Baroni F, Formigli L, Zurdo JS, Taddei N, Ramponi G, Dobson CM, Stefani M. Nature. 2002; 416:507. [PubMed: 11932737] Dobson CM. Nature. 2003; 426:884. [PubMed: 14685248]

[6]. Kayed R, Head E, Thompson JL, McIntire TM, Milton SC, Cotman CW, Glabe CG. Science. 2003; 300:486. [PubMed: 12702875]

[7]. Kuang Y, Xu B. Angew. Chem.-Int. Edit. 2013; 52:6944.

[8]. Zhang Y, Kuang Y, Gao YA, Xu B. Langmuir. 2011; 27:529. [PubMed: 20608718]

[9]. Reches M, Gazit E. Science. 2003; 300:625. [PubMed: 12714741]

[10]. Ma ML, Kuang Y, Gao Y, Zhang Y, Gao P, Xu B. J Am Chem Soc. 2010; 132:2719. [PubMed: 20131781]

[11]. Greenfield NJ. Nat. Protoc. 2006; 1:2876. [PubMed: 17406547]

[12]. Palecz B. J. Therm. Anal. Calorim. 1998; 54:257.

[13]. Pastor MT, Kummerer N, Schubert V, Esteras-Chopo A, Dotti CG, de la Paz ML, Serrano L. J. Mol. Biol. 2008; 375:695. [PubMed: 18036611]

[14]. Lincz LF. Immunol. Cell Biol. 1998; 76:1. [PubMed: 9553771]

[15]. Fogh J, Fogh JM, Orfeo T. Journal of the National Cancer Institute. 1977; 59:221. [PubMed: 327080]

[16]. Liebmann JE, Cook JA, Lipschultz C, Teague D, Fisher J, Mitchell JB. Br. J. Cancer. 1993; 68:1104. [PubMed: 7903152]

[17]. Zhao PQ, Wang HJ, Yu M, Liao ZY, Wang XH, Zhang F, Ji W, Wu B, Han JH, Zhang HC, Wang HQ, Chang J, Niu RF. Eur. J. Pharm. Biopharm. 2012; 81:248. [PubMed: 22446630]

[18]. D.L. H. J Am. Assoc. Lab. Anim. Sci. 2007:111.

[19]. Griffin, JP.; O'Grady, J. The textbook of pharmaceutical medicine. Wiley-Blackwell; 2006.

[20]. Kuang Y, Yuan D, Zhang Y, Kao A, Du XW, Xu B. Rsc Adv. 2013; 3:7704. [PubMed: 23766892]

[21]. Li XM, Du XW, Li JY, Gao Y, Pan Y, Shi JF, Zhou N, Xu B. Langmuir. 2012; 28:13512. [PubMed: 22906360]

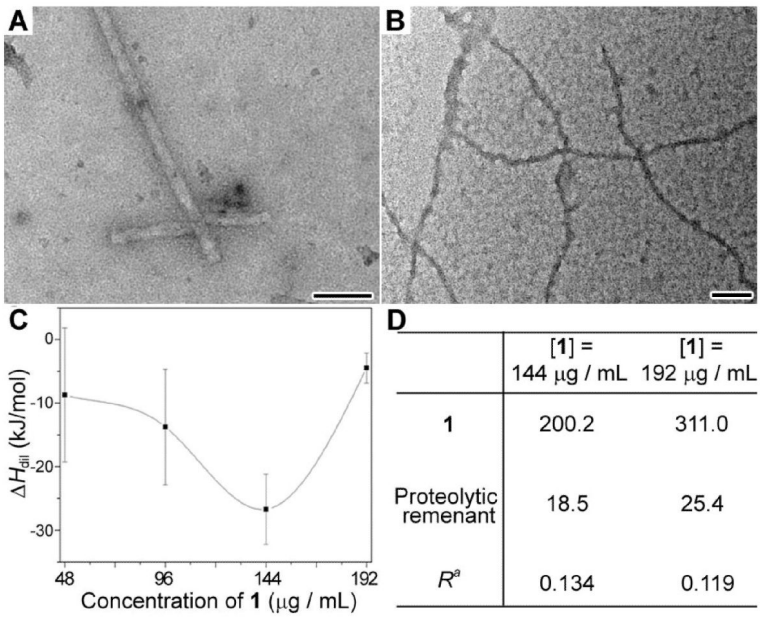

	[1] = 144 μg / mL	[1] = 192 μg / mL
1	200.2	311.0
Proteolytic remenant	18.5	25.4
R^a	0.134	0.119

Figure 1.

Characterization of the nanofibrils formed by **1**. (A) Negative stained TEM image of the nanofibrils in PBS buffer ([**1**] = 192 μg/mL). (B) Negative stained TEM image of the nanofibrils in complete culture medium ([**1**] = 192 μg/mL). Scale bar = 100 nm. (C) Plot of the heat release, measured by ITC, from the dilution of the solution of **1** at different concentrations. Data are presented as mean ± SD of 3 individual experiments. (D) Intracellular concentration (in the unit of μg/mL) of **1** and the proteolytic remnant of **1** in HeLa cells treated by **1** at 144 or 192 μg/mL measured and quantified by LC-MS. [a]*R* indicates the molar ratio of the intracellular concentration of the proteolytic remnant to the intracellular concentration of **1**.

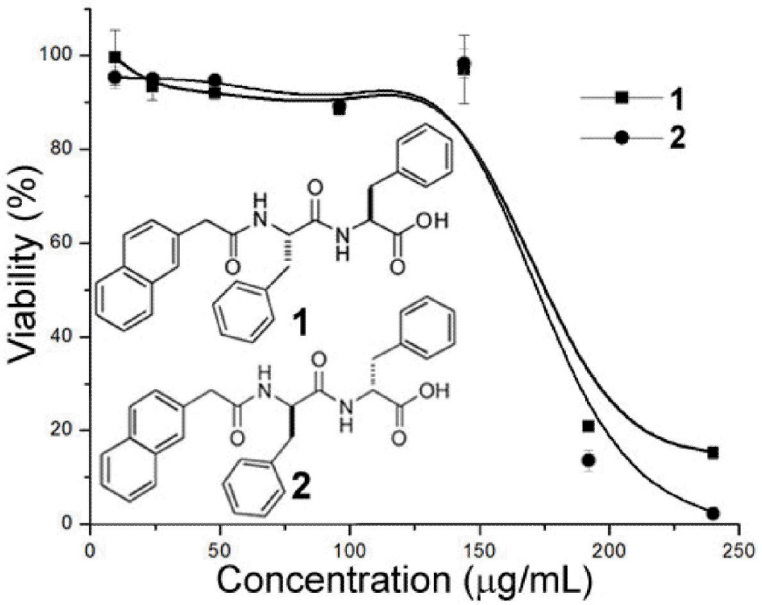

Figure 2.

Chemical structures and 48 h MTT cell viability tests of **1** and its enantiomer **2** towards HeLa cells.

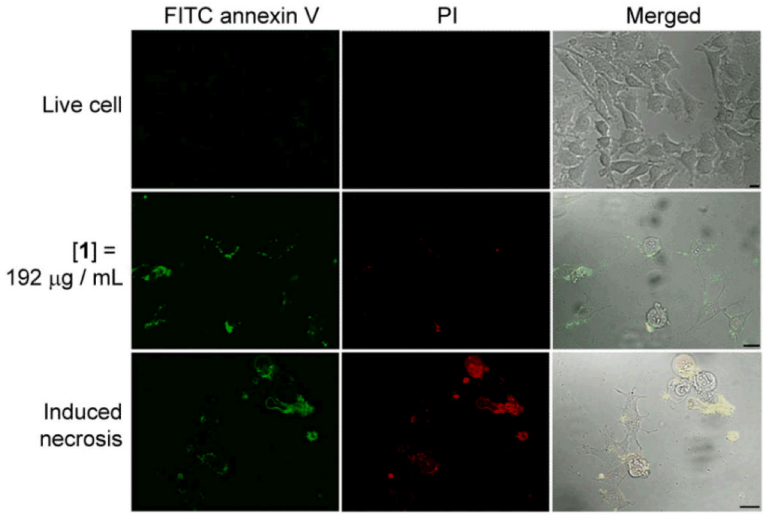

Figure 3.

Confocal images of FITC annexin V (green) and PI (red) stained HeLa cells. Live cells are untreated HeLa cells; induced necrotic HeLa cells are pre-treated by DMSO. Scale bar = 20 μm.

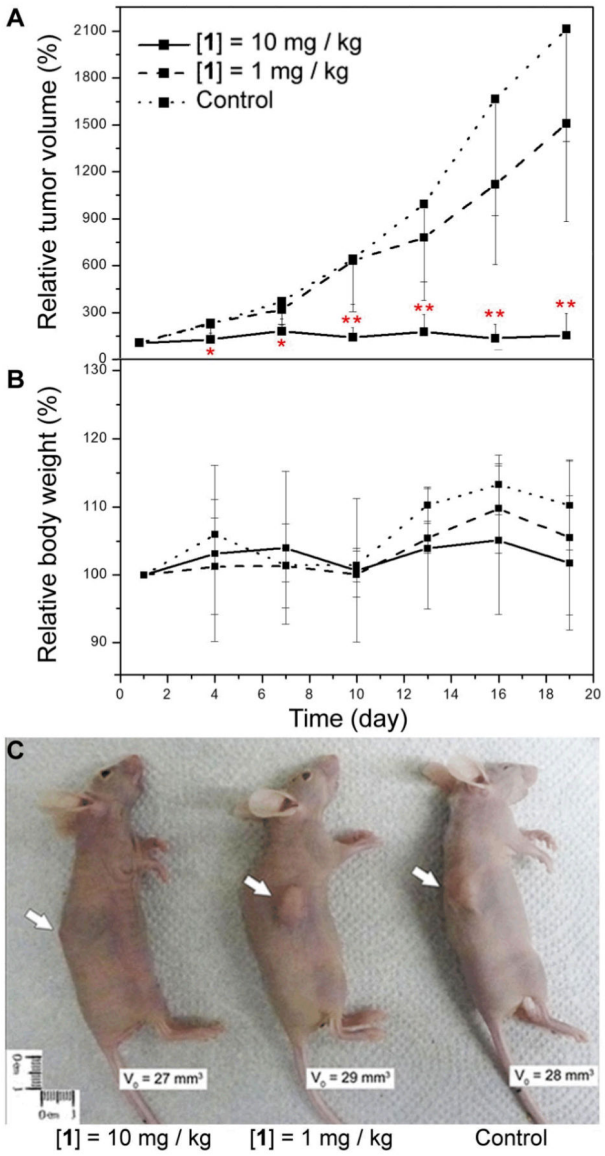

Figure 4.

Inhibitory effect of nanofibrils of **1** towards xenograft HeLa tumor on nu/nu mice. (A) Tumor progression curves of mice bearing HeLa tumors. 0.1 mL of **1** at 2.4 mg/mL or 0.24 mg/mL in PBS buffers or just PBS buffer as control was injected subcutaneously and peritumorally in every three days (six doses, starting day 1). Data are shown as mean ± SD (n = 9 for the group treated by 10 mg/kg of **1**, n = 4 for the group treated by 1 mg/kg of **1**, and n = 6 for control group). *$p < 0.05$, **$p < 0.01$ by Student's t test. (B) The change of the body weights of mice during the treatment. (C) Representative image shows mice bearing tumors with similar initial volume (V_0) from each group on 19th day of treatment. White arrows point at tumor.

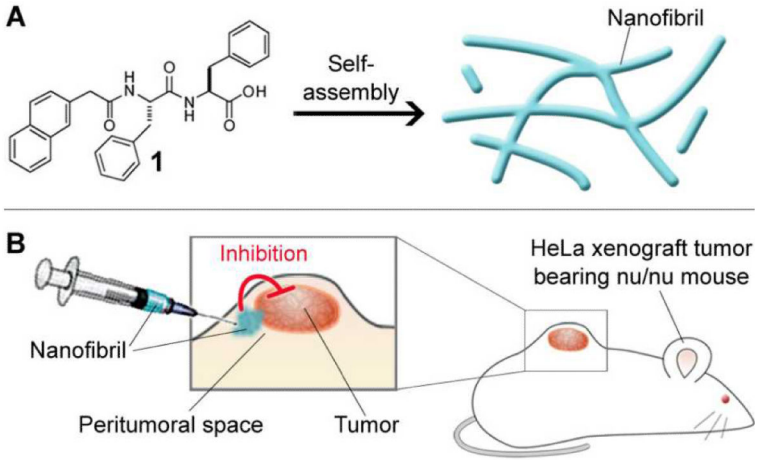

Scheme 1.

Self-assembly of **1** and the inhibition of tumor progression by the nanofibrils of **1**. (A) **1** self-assembles to form molecular nanofibrils. (B) Injection of the nanofibrils into the peritumoral space of xenograft HeLa tumor in nu/nu mouse inhibits the tumor progression.